

ABO EL-MAGD, N.F., BARBOSA, P.O., NICK, J., COVALERO, V., GRIGNETTI, G. and BERMANO, G. 2022. Selenium, as selenite, prevents adipogenesis by modulating selenoproteins gene expression and oxidative stress-related genes. *Nutrition* [online], 93, article 111424. Available from: <https://doi.org/10.1016/j.nut.2021.111424>

# Selenium, as selenite, prevents adipogenesis by modulating selenoproteins gene expression and oxidative stress-related genes.

ABO EL-MAGD, N.F., BARBOSA, P.O., NICK, J., COVALERO, V.,  
GRIGNETTI, G. and BERMANO, G.

2022

© 2021 The Author(s). Published by Elsevier Inc.

  
**OpenAIR**  
@RGU

This document was downloaded from  
<https://openair.rgu.ac.uk>





## Basic nutritional investigation

## Selenium, as selenite, prevents adipogenesis by modulating selenoproteins gene expression and oxidative stress–related genes



Nada F. Abo El-Magd Ph.D.<sup>a,b</sup>, Priscila O. Barbosa Ph.D.<sup>a</sup>, Julia Nick B.Sc.<sup>a</sup>, Viviana Covalero B.Sc.<sup>a</sup>, Giacomo Grignetti M.Sc.<sup>a</sup>, Giovanna Bermano Ph.D.<sup>a,\*</sup>

<sup>a</sup> Centre for Obesity Research and Education, School of Pharmacy and Life Sciences, Robert Gordon University, Aberdeen, United Kingdom

<sup>b</sup> Biochemistry Department, Faculty of Pharmacy, Mansoura University, Mansoura, Egypt

## ARTICLE INFO

## Article History:

Received 18 December 2020

Received in revised form 2 July 2021

Accepted 14 July 2021

## Keywords:

Adipocytes  
Antioxidant  
Obesity  
Selenium  
Selenoproteins

## ABSTRACT

**Objectives:** The aim of this study was to assess the effect of the micronutrient selenium, as inorganic selenite, on adipocytes differentiation, and to identify underlying molecular mechanisms to advance the understanding of basic cellular mechanisms associated with adipogenesis.

**Methods:** The effect of sodium selenite ( $\text{Na}_2\text{SeO}_3$ ) on cell viability (bromide 3-[4,5-dimethylthiazol-2-yl]-2,5-difeniltetrazol [MTT] assay) in preadipocytes, lipid accumulation (oil red O [ORO] assay) and intracellular reactive oxygen species (ROS, [NBT assay]) in mature adipocytes, as well as explore molecular mechanisms via gene expression analyses (real-time quantitative polymerase chain reaction), before and after differentiation, was investigated using 3T3-L1 murine preadipocytes.

**Results:** Selenite (100, 200, and 400 nM) significantly decreased lipid accumulation during differentiation compared with untreated adipocytes ( $P < 0.05$ , 0.001, and 0.01, respectively). Preadipocytes exposure (48 h) to selenite caused an increase in glutathione peroxidase 1 (*Gpx1*) gene expression in a dose-dependent manner. Adipogenesis significantly increased intracellular reactive oxygen species levels ( $P < 0.05$ ) while decreasing gene expression of antioxidant enzymes (*Gpx1*:  $P < 0.05$ ) and significantly increasing gene expression of regulators of lipid catabolism (type II iodothyronine deiodinase [*Dio2*],  $P < 0.01$ ) and markers of differentiation (eg, selenium-binding protein 1 [*Selenbp1*], peroxisome proliferator activated receptor gamma [*Pparg*], CCAAT/enhancer binding protein alpha [*Cebpa*], and fatty acid binding protein 4 [*Fab4*]) compared with preadipocytes ( $P < 0.01$ , 0.01, 0.01, and 0.001, respectively). Selenite exposure (200 nM) caused a significant increase in *Gpx1*, selenoprotein W (*Selenow*) and selenoprotein P (*Selenop*) gene expression, in adipocytes compared with untreated ones ( $P < 0.01$ , 0.001, and 0.05, respectively) with a significant decrease in heme oxygenase 1 (*Ho-1*), cyclooxygenase 2 (*Cox2*), *Dio2*, and *Fabp4* gene expression ( $P < 0.001$ , 0.05, 0.05, and 0.01, respectively).

**Conclusions:** Selenium, as selenite, prevented adipogenesis through increasing antioxidant selenoprotein expression, leading to decreased inflammatory markers and, subsequently, to a decrease in differentiation and lipid deposition. These findings, if demonstrated *in vivo*, could provide valuable data for novel dietary approaches to prevent obesity.

© 2021 The Author(s). Published by Elsevier Inc. This is an open access article under the CC BY license (<http://creativecommons.org/licenses/by/4.0/>)

## Introduction

Obesity is a chronic and progressive disease that affects a significant proportion of the world's population. Obesity is a major risk factor for type 2 diabetes, metabolic syndrome a hypertension, stroke, and cardiovascular disease [1–3]. Previous clinical studies have identified a correlation between obesity and systemic oxidative stress [4], and preliminary studies in animal or *in vitro* models

acknowledged a significant role of antioxidant enzymes in regulating adipogenesis [5,6].

Adipogenesis plays a crucial role in the increase of adipose mass and obesity development [7]. During this process, cells undergo biochemical and morphologic changes, which are partly associated with or driven by oxidative stress. Therefore, oxidative stress plays a promoting role in lipid accumulation, as previously demonstrated in *in vitro* studies where both oxidative and endoplasmic reticulum stress induced lipid droplet accumulation in a hepatoma cell line and cultured hepatocytes [8–10]. Moreover, reactive oxygen species (ROS) have been shown to augment adipocytes

\*Corresponding author. Tel.: +44 (0)1224262885.

E-mail address: [g.bermano@rgu.ac.uk](mailto:g.bermano@rgu.ac.uk) (G. Bermano).

differentiation and lipid accumulation in 3T3-L1 cells, a widely used cell model to study basic cellular mechanisms associated with adipogenesis and obesity, due to their potential to differentiate from fibroblasts into mature adipocytes [11]. Maintenance of redox homeostasis is important for adipogenesis regulation and obesity prevention and is regulated through numerous genes, including nuclear factor erythroid 2 related factor 2 (*Nrf2*), heme oxygenase 1 (*Ho-1*), glutathione S-transferase, superoxide dismutase, catalase, and selenoproteins such as glutathione peroxidases (*Gpxs*) and thioredoxin reductase 1 (*Txnrd1*) [12].

Deficiencies in micronutrients, such as vitamins and trace elements, can contribute to the development of impaired antioxidant defenses potentially involved in the pathogenesis of obesity and associated diseases by modulating redox homeostasis. Lower selenium and zinc levels have been observed in obese children [13,14], especially with central obesity and morbidly obese patients present magnesium, selenium, iron, and zinc deficiencies [15]. These results may suggest that, in the obese population, inadequate concentrations of vitamins and minerals may cause the observed impaired antioxidant defense [5]. However, further studies are required to elucidate associations between micronutrients levels and obesity. Although supplementation with minerals and vitamins may be beneficial, in relation to selenium supplementation, a recent review of the literature showed a counterpoint about high doses of selenium and its relationship with the development of obesity in the upregulation of adipocyte-specific genes [16]. Therefore, understanding the participation of selenium in the redox metabolism and adipocytes differentiation is a promising area of research and of clinical relevance, as well as essential for safe and targeted dietary guidance. Moreover, the high expression of selenium-containing proteins in adipose tissue in both healthy and obese conditions [17,18] is indicative of the significant role of selenium in adipocytes biology, and warrants further research.

Selenium is an essential micronutrient that has potent anti-oxidative and anti-inflammatory properties [19,20]. Selenium acts mainly through selenocysteine-containing proteins, and is incorporated into selenocysteine amino acid in the catalytic site of enzymatically active selenoproteins, thus representing an essential component of selenoproteins [21,22]. Several selenoproteins, such as thioredoxin reductase isoenzymes (TXNRD1 and TXNRD2), glutathione peroxidases isoenzymes (GPX1–4), selenoprotein P (SELENO P), selenoprotein S (SELENOS), and selenoprotein W (SELENOW), play an important role in the cellular defense systems against oxidative stress [23,24]. SELENOW has been shown to have an important role in protecting immune organs from inflammatory injury through the regulation of inflammation-related genes [25]. More specifically to adipose tissue and in addition to the above-mentioned selenoproteins, iodothyronine deiodinases (DIOs) are highly expressed, and their expression and activity is modulated by adipose tissue remodeling in obesity. In particular, increased expression of type II iodothyronine deiodinase (DIO2) has been tightly associated with reduced lipid catabolism and mitochondrial dysfunction [26]. Even if not a selenoprotein, selenium-binding protein 1 (SELENBP1) has been shown recently to be a marker of mature adipocytes and a catalyst to the oxidation of methanethiol into hydrogen peroxide and hydrogen sulphide, which are key signaling molecules for adipocyte differentiation [27].

The micronutrient selenium has been suggested to have anti-inflammatory and anti-oxidative properties through its incorporation in selenoproteins, but the exact mechanisms by which selenium may affect adipogenesis are not clear. The present study used 3T3-L1 cells to advance the understanding of the basic cellular mechanisms associated with adipogenesis, and aimed to identify how selenium may affect differentiation into mature

adipocytes and its underlying molecular mechanisms. The effect of selenium, as inorganic selenite, on gene expression of several selenoproteins (eg, *Gpx1*, *Gpx4*, *Selenop*, *Selenos*, *Selenow* and *Dio2*), markers of adipocytes differentiation (eg, *Selenbp1*, peroxisome proliferator activated receptor gamma [*Pparg*], CCAAT/enhancer binding protein alpha [*Cebpa*] and fatty acid binding protein 4 [*Fabp4*]), redox and energy metabolism regulators (*Nrf2*, *Ho-1*, and uncoupling protein 2 [*Ucp2*]), and inflammation (eg, cyclooxygenase 2 [*Cox2*]) has been determined in 3T3-L1 pre- and mature adipocytes cultured in different concentrations of selenium.

## Methods

### Cell culture

For this study, 3T3-L1 preadipocytes were purchased from European Collection of Authenticated Cell Cultures (distributed via Sigma Aldrich, United Kingdom; number: 86052701, lot: 130030), and cultured at 37°C/8% CO<sub>2</sub> in Dulbecco's modified Eagle's medium (DMEM + Glutamax, containing 4.5 g/L glucose + pyruvate [Gibco cat no. 31966-021]), supplemented with 1% penicillin/streptomycin (Gibco, cat no. 15140-122), and 10% newborn calf serum (NBCS, Gibco, cat no. 26010). The 3T3-L1 cells were used until passage 10.

### Cell viability assay

To evaluate the effect of different concentrations of sodium selenite (Na<sub>2</sub>SeO<sub>3</sub>; 50, 100, 200, and 400 nM) on cell viability, a bromide 3-(4,5-dimethylthiazol-2-yl)-2,5-diphenyltetrazol (MTT) assay was used. The assay is based on the presence of mitochondrial enzymes in viable cells that reduce MTT to produce purple formazan crystals.

As previously described [28], cells were seeded at a concentration of  $3.5 \times 10^3$  or  $5 \times 10^3$  cells/well in 96 well plates, and incubated for 24 h before changing medium containing different sodium selenite concentrations (50, 100, 200, and 400 nM). After 48 h, the treatment media were removed, and 100  $\mu$ L MTT (1 mg/mL in complete medium [DMEM medium supplemented with 10% NBCS]) was added to each well and incubated for 4 h at 37°C in the dark. The MTT solution was removed, and 200  $\mu$ L dimethyl sulfoxide (DMSO) was added to each well to solubilize formazan crystals for 30 min in the dark on a shaker. Subsequently, absorbance was measured at 560 nM.

### Cell differentiation and treatment protocols

Differentiation of the cells was carried out with two different protocols as described and summarized in the diagram in Figure 1.

For protocol 1, cells seeded at a concentration of  $2 \times 10^4$  cells/well in 24 wells plates were allowed to grow to confluence. Forty-eight hours after confluence (day 0), cells were treated with a DMEM medium containing a hormone mixture (MDI) and 10% fetal bovine serum (FBS, Gibco, cat no. 10500-064) for 2 d. The hormone mixture was composed of 0.5 mM 3-isobutyl-1-methylxanthine (IBMX), 1  $\mu$ M dexamethasone, 1  $\mu$ g/mL insulin, and 1  $\mu$ M rosiglitazone. On day 2, the culture medium was replenished with DMEM (10% FBS), supplemented only with 1  $\mu$ g/mL insulin for 5 d. On day 7, the culture medium was replenished with DMEM (10% FBS) for 2 d (according to published protocol [29]).

For protocol 2, the cells were cultured similarly to protocol 1 apart from the following changes: MDI was composed of 0.5 mM IBMX, 1  $\mu$ M dexamethasone, and 1  $\mu$ g/mL insulin only, and the duration of the incubation with the insulin medium was reduced to 3 d and subsequently replenished at day 5 with DMEM (10% FBS) for 2 d (according to published protocol [30]).

Different treatments were used during the differentiation protocol, including 10 mM N-acetyl-L-cysteine (NAC, positive control) and different concentrations of sodium selenite (100, 200, and 400 nM) as reported in the diagram in Figure 1.

### Lipid content

To assess the progress of differentiation, lipid accumulation was measured using oil red O (ORO) dye. ORO staining was performed according to the following protocol [31]: at the end of the differentiation protocol, the medium was removed and cells were washed with phosphate-buffered saline (PBS) before incubating cells with 10% formalin buffered saline for 30 min. Cells were washed two times with PBS, and subsequently incubated with 60% isopropanol for 5 min. Isopropanol solution was removed, and cells were incubated with ORO working solution (0.5% stock solution mixed with Milli-Q water at a ratio of 3:2) for 1 h at room temperature in the dark. Excess ORO was removed by washing three times with double-distilled water. Isopropanol was added to each well to solubilize ORO, and incubated for 15 min in the dark on a shaker. Subsequently, absorbance was measured at 590 nm. The % ORO staining was calculated relative to the control (adipocytes).

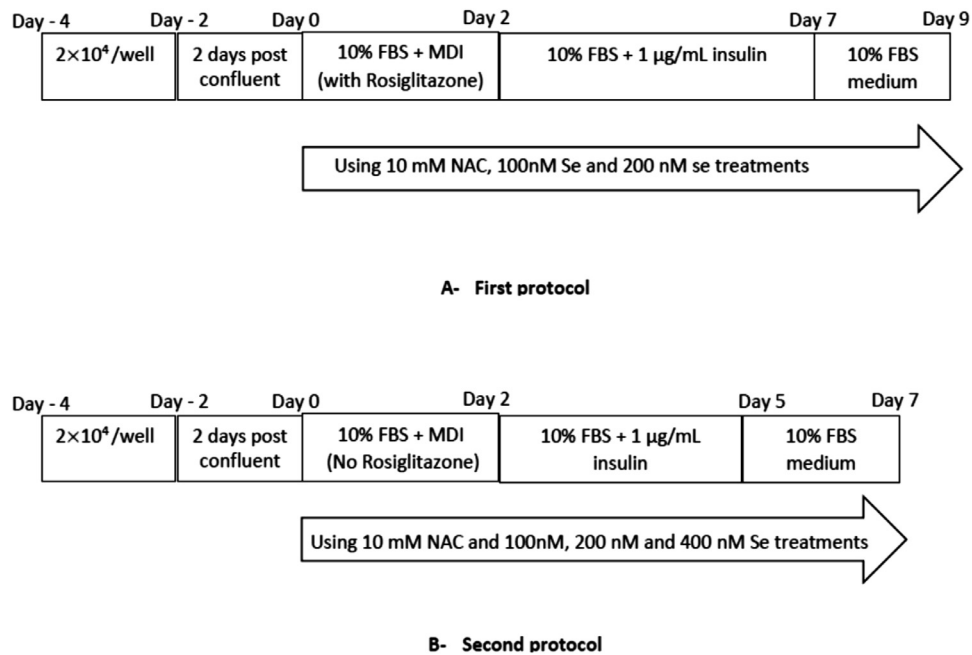


**Fig. 1.** Differentiation and treatment protocols used in the study. FBS, fetal bovine serum; MDI, hormone mixture; NAC, N-acetyl-L-cysteine; Se, sodium selenite.

#### Intracellular reactive oxygen species levels

To assess the amount of ROS present within cells during differentiation and after sodium selenite treatment, the nitroblue tetrazolium (NBT) assay was performed according to the following protocol [32] with small modifications. In brief, at the end of the differentiation protocol, the medium was removed, and replaced with 0.5 mL NBT solution (0.2% NBT in PBS) per well. Cells were incubated at 37°C in the dark for 90 min. Then, the NBT solution was removed, and cells were washed twice with methanol and left to air dry for few minutes. Subsequently, the NBT deposited inside the cells was dissolved, first by adding 240 µL 2 M KOH to solubilize cell membranes and then by adding 280 µL DMSO to dissolve blue formazan with gentle shaking for 20 min at room temperature in the dark. Absorbance was measured at 630 nm. The % NBT staining was calculated relative to the control (adipocytes).

#### Gene expression

RNA was extracted from either preadipocytes treated for 48 h with different concentrations of sodium selenite or from mature adipocytes treated with different concentrations of sodium selenite during the differentiation stages. Total RNA was isolated from cells using the TRI Reagent solution (Ambion, United Kingdom) per manufacturer's guidelines. Subsequently, the RNA pellet was dissolved in

nuclease-free water, and RNA concentration and purity were assessed by measuring absorbance at 260/280 nm. One hundred ng of total RNA was used for cDNA synthesis using SuperScript III Reverse Transcriptase (Invitrogen, United Kingdom) and random hexamers as primers (Promega, United Kingdom).

Real-time polymerase chain reaction (PCR) was performed using the SYBR Green PCR Master Mix kit (Primer Design, United Kingdom), as recommended by the manufacturer, and 0.25 µM of forward and reverse primers. Primers were designed using PubMed (Entrez Gene) and Premier Biosoft (Palo Alto, CA; Table 1). mRNA levels were quantified using the comparative threshold cycle ( $2^{-\Delta\Delta CT}$ ) method. The data were normalized to  $\beta 2$  microglobulin (*B2m*) RNA to account for differences in reverse transcriptase efficiencies and the amount of template in the reaction mixtures.

#### Statistical analysis

All results were expressed as mean  $\pm$  standard error of the mean (mean  $\pm$  SE). Student's *t* test was used to analyze statistically significant differences between the two groups. A one-way analysis of variance, followed by Tukey or Dunn's tests according to the distribution of the data, was also used to analyze statistically significant differences between the groups. *P*-values of  $< 0.05$  were considered significant. The statistical analysis was conducted using GraphPad Prism software, version 7.0 (GraphPad Software; San Diego, CA).

**Table 1**  
Sequence of primers used for quantitative polymerase chain reaction

Gene	Forward primer	Reverse primer	Product size (bp)
<i>B2m</i>	TGGTCTTTCTGGTGCTGTCT	GGATTTCATGTGAGGCGGG	153
<i>Cebpa</i>	TGAAGGAACCTGAAGCACA	TCAGAGCAAAACCAAAACAA	201
<i>Cox2</i> [33]	AAGCGAGGACCTGGGTTC	AAGCGCAGTTTATGTGTCTGT	96
<i>Dio2</i>	ATGGGACTCCTCAGCGTAGAC	ACTCTCCGCGAGTGACTT	150
<i>Fabp4</i>	ATGATCATCAGCGTAAATGG	GCCTTTCATAACACATTCCA	245
<i>Gpx1</i>	CAGGAGAATGGCAAGATGA	GAAGGTAAGAGCGGGTGAG	135
<i>Gpx4</i> [34]	GCTGGGAAATGCCATCAAATGGA	ACGGCAGGTCCTCTCTATCAC	115
<i>Ho-1</i>	CGCTACTGGGTGACCTCTC	TGTTTGAACCTTGGTGGGCT	134
<i>Nrf2</i>	GGAAGTGTCAAACAGAACCGC	GACCAGGACTCACGGAACT	154
<i>Pparg</i>	GTCTGTGGGGATAAAGCATC	CTGATGGCATTGTGAGACAT	205
<i>Selenbp1</i> [27]	TGAGCCTCTGCTCGTTCC	TGGACCACACTTTGTGCATT	88
<i>Selenop</i> [34]	CTCATCTATGACAGATGTGGCCGT	AAGACTCGTGAGATTGCAGTTCC	137
<i>Selenos</i> [34]	GAAGGCCTCAGGAAGATGTT	GTCTCCAGGAGCAGGTCCA	137
<i>Selenow</i> [34]	ATGCCTGGACATTTGTGGCGA	GCAGCTTTGATGGCGTCCAC	153
<i>Ucp2</i>	TAAGTCTTTCGTCTCCAGCC	GCTTCTCTAAAGGTGCTCGTTT	99

*B2m*, beta 2 microglobulin; *Cebpa*, CCAAT/enhancer binding protein alpha; *Cox2*, cyclooxygenase 2; *Dio2*, type II iodothyronine deiodinase; *Fabp4*, fatty acid binding protein 4; *Gpx1*, glutathione peroxidase 1; *Gpx4*, glutathione peroxidase 4; *Ho-1*, heme oxygenase 1; *Nrf2*, nuclear factor erythroid 2 related factor 2; *Pparg*, peroxisome proliferator activated receptor gamma; *Selenbp1*, selenium-binding protein 1; *Selenop*, selenoprotein P; *Selenos*, selenoprotein S; *Selenow*, selenoprotein W; *Ucp2*, uncoupling protein 2.

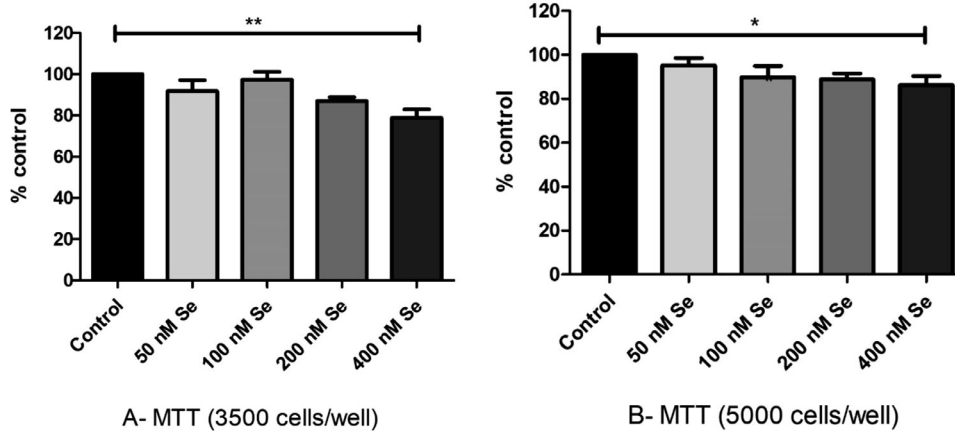


**Fig. 2.** Effect of selenite on cell viability. Cell viability was assessed in 3T3-L1 cells at a concentration of either (A) 3500 cells/well ( $n = 6$ ), or (B) 5000 cells/well ( $n = 7$ ) after exposure to different concentrations of sodium selenite (50, 100, 200, and 400 nM) for 48 h. Data are expressed as percentage of untreated cells (control). \* $P < 0.05$ ; \*\* $P < 0.01$  versus control. MTT, bromide 3-[4,5-dimethylthiazol-2-yl]-2,5-difeniltetrazol; Se, sodium selenite.

## Results

### Selenite affects preadipocyte cell viability at high concentrations

Concentrations of 50, 100, and 200 nM sodium selenite did not affect cell viability when tested against 3500 or 5000 cells/well, but 400 nM induced a significant decrease in cell viability (21%,  $P < 0.01$ ; and 14%,  $P < 0.05$ , when cells were seeded at 3500 and 5000 cells/well, respectively; Fig. 2).

### Selenite supplementation during differentiation affects lipid accumulation in protocol-dependent manner

According to protocol 1, which includes the use of rosiglitazone in the differentiation process, different amounts of selenite did not cause significant changes in lipid accumulation, but 10 mM NAC (positive control) caused a 29% significant decrease in ORO staining compared with untreated adipocytes (control;  $P < 0.01$ ; Fig. 3A).

NAC was used as a positive control for adipogenesis inhibition, because NAC is a well-known strong antioxidant and has been used to hinder 3T3-L1 differentiation in several studies [35–37]. NAC was used as a positive control in cytotoxicity assays without affecting cell viability at the concentrations tested (data not shown).

While using protocol 2, the addition of 10 mM NAC and 100, 200, or 400 nM sodium selenite during all stages of differentiation induced a significant decrease (13%, 14%, 19%, and 19%, respectively;  $P < 0.05$ , 0.05, 0.001, and 0.01, respectively) in ORO staining compared with untreated adipocytes (control; Fig. 3B).

### Selenite differentially affects Gpx1 and Gpx4 gene expression in preadipocytes

The effect of 48 h treatment of preadipocytes with different doses of sodium selenite on the expression of *Gpx1* and *Gpx4* genes was investigated. Selenite induced an increase in *Gpx1* expression

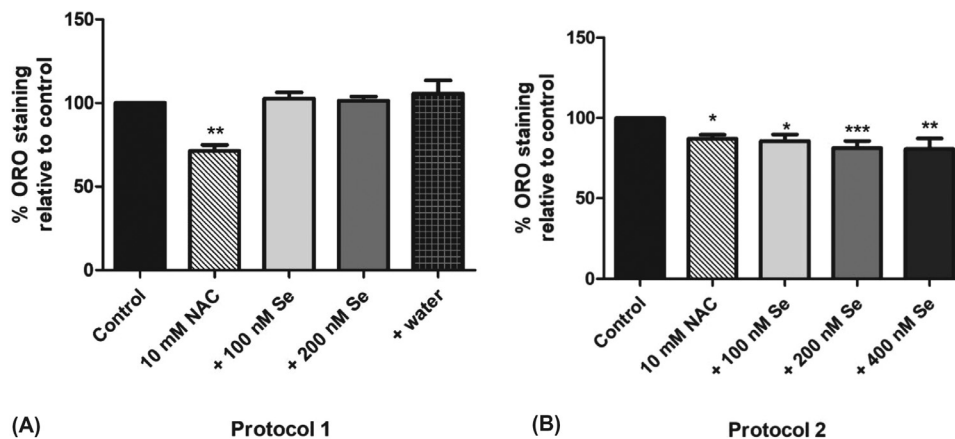


**Fig. 3.** Effect of selenite on lipid accumulation. Lipid accumulation was detected in adipocytes by ORO staining in the (A) presence of rosiglitazone ( $n = 6$ ), and (B) absence in MDI ( $n = 6$ ) after incubation with 10 mM NAC, and 100, 200, and 400 nM sodium selenite. Water was used to prepare sodium selenite solutions and used as vehicle control (A). Data are expressed as percentage of untreated adipocytes (control). \* $P < 0.05$ ; \*\* $P < 0.01$ ; \*\*\* $P < 0.001$  versus control group. NAC, n-acetyl-L-cysteine; ORO, oil red O; Se, sodium selenite.



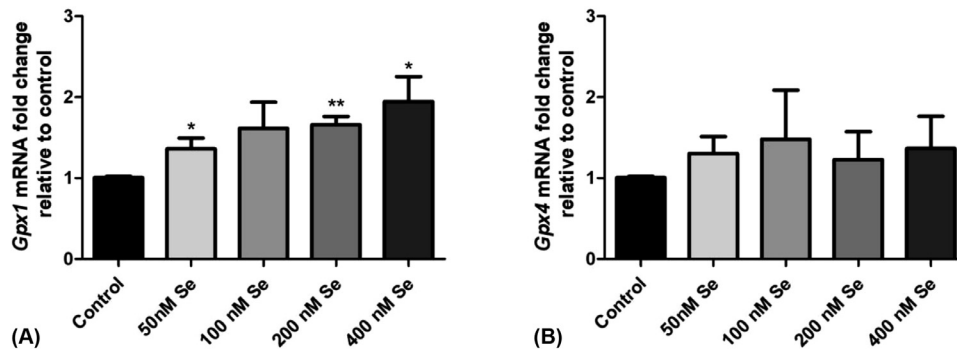


**Fig. 4.** Effect of selenite on *Gpx1* and *Gpx4* expression in preadipocytes. (A) *Gpx1* and (B) *Gpx4* mRNA abundance in preadipocytes exposed to 50, 100, 200 nM and 400 nM sodium selenite for 48 h (n = 4). Data are expressed as fold change compared with untreated preadipocytes (control). \* $P < 0.05$ ; \*\* $P < 0.01$  versus control group. *Gpx1*, glutathione peroxidase 1; *Gpx4*, glutathione peroxidase 4; Se, sodium selenite.

in a dose-dependent manner (Fig. 4A). In particular, 50, 200, and 400 nM sodium selenite caused a significant increase in *Gpx1* expression compared with untreated cells. *Gpx1* expression increased 1.4-fold ( $P < 0.05$ ), 1.7-fold ( $P < 0.01$ ), and 1.9-fold ( $P < 0.05$ ) in cells incubated with 50, 200, and 400 nM of sodium selenite, respectively. No significant changes in *Gpx4* gene expression were observed with different selenite doses (Fig. 4B).

#### Selenite supplementation during differentiation affects intracellular reactive oxygen species levels

Because 200 nM sodium selenite induced a significant decrease in lipid accumulation (Fig. 3B) without causing a significant change in cell viability (Figs. 2A and B), 200 nM sodium selenite supplementation was chosen as the optimal concentration to study the effects of ROS levels within cells and, subsequently, on gene expression of markers of antioxidant status, redox and energy metabolism regulators, and inflammation. The differentiation process caused a 37% increase ( $P < 0.01$ ) in ROS levels measured by NBT assay (Fig. 5) compared with preadipocytes cultured for the same length of time as in the differentiation protocol (protocol 2, 7 d). However, the addition of 200 nM sodium selenite during the differentiation process (day

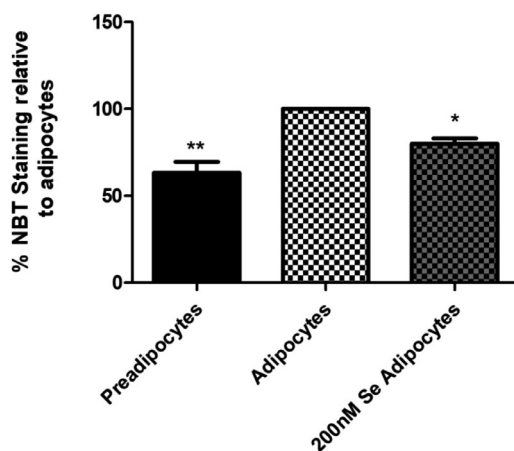


**Fig. 5.** Effect of selenite on intracellular ROS levels. ROS levels were detected in preadipocytes, adipocytes, and adipocytes supplemented with 200 nM sodium selenite (200 nM Se adipocytes) by NBT staining (n = 3). Data are expressed as percentage of untreated adipocytes. \* $P < 0.05$ ; \*\* $P < 0.01$  versus adipocytes. NBT, nitroblue tetrazolium; Se, sodium selenite.

0–7) caused a significant decrease in ROS (20%;  $P < 0.05$ ) compared with untreated adipocytes.

#### Selenite differentially affects expression of markers of antioxidant status in preadipocyte

Exposure of 3T3-L1 preadipocytes for 7 d to 200 nM sodium selenite induced a significant increase in *Selenow* mRNA ( $P < 0.05$ ) compared with untreated cells, but no other significant differences were observed for any of the genes tested (Fig. 6).

#### Differentiation affects expression of markers of antioxidant status and energy metabolism regulators

The differentiation protocol that involved the use of hormone mixture without rosiglitazone and exposure to insulin for 3 d was used to further investigate the molecular changes that occur during differentiation on biomarkers of adipocytes differentiation, antioxidant status, redox metabolism regulators, and inflammation. The expression of *Gpx1* was significantly decreased (0.4-fold;

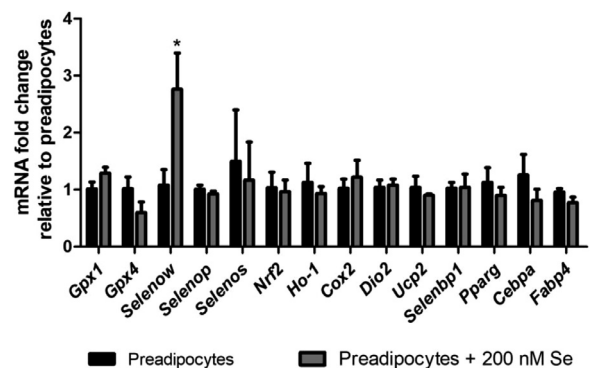


**Fig. 6.** Effect of 7 d exposure to 200 nM sodium selenite on gene expression in preadipocytes. *Gpx1*, *Gpx4*, *Selenow*, *Selenop*, *Selenos*, *Nrf2*, *Ho-1*, *Cox2*, *Dio2*, *Ucp2*, *Selenbp1*, *Pparg*, *Cebpa* and *Fabp4* gene expression in preadipocytes exposed to 200 nM sodium selenite for 7 d (preadipocytes + 200 nM Se; n = 3–7). Data are expressed as fold change compared with untreated preadipocytes (black bar). \* $P < 0.05$  versus preadipocytes. *Cebpa*, CCAAT/enhancer binding protein alpha; *Cox2*, cyclooxygenase 2; *Dio2*, type II iodothyronine deiodinase; *Fabp4*, fatty acid binding protein 4; *Gpx1*, glutathione peroxidase 1; *Gpx4*, glutathione peroxidase 4; *Ho-1*, heme oxygenase 1; *Nrf2*, nuclear factor erythroid 2 related factor 2; *Pparg*, peroxisome proliferator activated receptor gamma; Se, sodium selenite; *Selenbp1*, selenium-binding protein P1; *Selenop*, selenoprotein P; *Selenos*, selenoprotein S; *Selenow*, selenoprotein W; *Ucp2*, uncoupling protein 2.

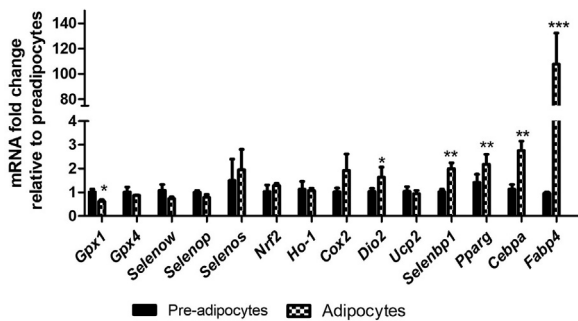


**Fig. 7.** Effect of differentiation on gene expression. *Gpx1*, *Gpx4*, *Selenow*, *Selenop*, *Selenos*, *Nrf2*, *Ho-1*, *Cox2*, *Dio2*, *Ucp2*, *Selenbp1*, *Pparg*, *Cebpa* and *Fabp4* gene expression in adipocytes ( $n = 3-7$ ). Data are expressed as fold change compared with preadipocytes (black bar). \* $P < 0.05$ ; \*\*\* $P < 0.001$  versus preadipocytes. *Cebpa*, CCAAT/enhancer binding protein alpha; *Cox2*, cyclooxygenase 2; *Dio2*, type II iodothyronine deiodinase; *Fabp4*, fatty acid binding protein 4; *Gpx1*, glutathione peroxidase 1; *Gpx4*, glutathione peroxidase 4; *Ho-1*, heme oxygenase 1; *Nrf2*, nuclear factor erythroid 2 related factor 2; *Pparg*, peroxisome proliferator activated receptor gamma; Se, sodium selenite; *Selenbp1*, selenium-binding protein P1; *Selenop*, selenoprotein P; *Selenos*, selenoprotein S; *Selenow*, selenoprotein W; *Ucp2*, uncoupling protein 2.

$P < 0.05$ ) in adipocytes compared with preadipocytes (Fig. 7), but the expression of *Selenow* had a similar decreasing trend without reaching significant difference (0.4-fold;  $P = 0.21$ ; Fig. 7). Expression of *Dio2*, *Selenbp1*, *Pparg*, *Cebpa* and *Fabp4* were significantly increased in adipocytes compared with preadipocytes (1.7-fold,  $P < 0.05$ ; 2.0-fold,  $P < 0.01$ ; 2.1-fold,  $P < 0.01$ ; 2.4-fold,  $P < 0.01$ ; and 112-fold,  $P < 0.001$ , respectively). The expression of *Cox2* showed a similar increasing trend in adipocytes compared with preadipocytes (1.9-fold) without reaching significant difference (Fig. 7).

#### *Selenite supplementation during differentiation affects expression of markers of antioxidant status, redox, and energy metabolism regulators, and inflammation in adipocytes*

The addition of 200 nM sodium selenite during the differentiation process (day 0–7) caused a significant increase in *Gpx1*, *Selenow* and *Selenop* mRNA expression (1.6-, 3.8-, 1.4-fold;  $P < 0.01$ , 0.001, and 0.05, respectively) compared with non-supplemented adipocytes (Fig. 8A). Selenite supplementation did not affect *Gpx4* (1.7-fold;  $P = 0.37$ ) or *Selenos* gene expression. However, selenite supplementation had a significant effect on *Ho-1* and *Cox2* gene expression by reducing their mRNA levels (0.4- and 0.5-fold, respectively) compared with non-supplemented adipocytes ( $P < 0.001$  and 0.05, respectively; Fig. 8B). *Nrf2* expression was not affected by sodium selenite supplementation.

With regard to biomarkers of energy metabolism and adipocytes differentiation, selenite supplementation reduced *Dio2* gene expression (0.3-fold;  $P < 0.05$ ) without affecting *Ucp2* gene expression. The expression of the *Fabp4* gene was significantly reduced by the addition of selenite (0.3-fold;  $P < 0.01$ ), and a similar trend was observed for *Cebpa* expression (0.5-fold) without reaching statistical difference (Fig. 8C). *Selenbp1* expression was not affected by selenite supplementation.

## Discussion

Obesity has been proposed to be modulated by oxidative stress and inflammation [5], whereas the micronutrient selenium has been suggested to have anti-inflammatory and anti-oxidative properties, which might be beneficial in preventing or reducing adipogenesis, therefore contributing to the management of

obesity. This study showed for the first time that supplementation with sodium selenite reduced adipocyte differentiation and lipid deposition in 3T3-L1 cells. Interestingly, the effects of selenium, as selenite, depended on the presence of rosiglitazone in induction medium, with selenite having no significant effect on lipid accumulation in the presence of rosiglitazone, but having sodium selenite at different concentrations (100, 200, and 400 nM) significantly decreased lipid deposition in adipocytes in the absence of rosiglitazone. These findings are consistent with the results of studies by Kobayashi et al. (2009), which used a different treatment protocol with selenium and stated that the presence of rosiglitazone in the medium inhibited the treatment potency of selenium [38], and Zhao et al. (2019), which suggested that rosiglitazone does not cause but can accelerate the differentiation process [11].

Understanding how selenium supplementation affects the gene expression of selenoproteins with antioxidant properties, such as GPX1, GPX4, SELENOW, SELENOP, and SELENOS, not only in preadipocytes but also in mature adipocytes, is important to identify the molecular mechanisms involved. Supplementation of preadipocytes with 200 nM sodium selenite for 48 h only increased *Gpx1* expression (Fig. 4A), whereas *Selenow* expression was increased after 7 d (Fig. 6). No effect was observed on *Gpx4*, *Selenop*, *Selenos* and *Dio2* expression. *Gpx1* expression was more affected than *Gpx4* expression, which may be explained by differences in *Gpx1* mRNA stability and biosynthesis compared with *Gpx4*, which is expressed more stably. *Gpx1* and *Gpx4* expression are differentially affected by selenium deficiency in the liver and colon of rats and mice, respectively, due to the increased stability of *Gpx4* mRNA and biosynthesis hierarchy [39]. *Gpx1* is considered the lowest in this hierarchy rank due to its rapid decline upon selenium deprivation, and is resynthesized with considerable delay upon selenium repletion [40–42]. Other selenoproteins, such as GPX4, GPX2, diiodinases, or thioredoxin reductases, rank high in the hierarchy. In general, the ranking of selenoproteins parallels the stability of their mRNA. However, no data are available on how selenium deficiency or supplementation may affect selenoproteins' hierarchy and mRNA stability in adipose tissue, and this is the first study suggesting a more rapid response of the *Gpx1* and *Selenow* gene to selenium supplementation for 2 d or 7 d, respectively.

The effect of selenium supplementation, as selenite, was also assessed on the expression of markers of adipocytes differentiation, redox, and energy metabolism regulators and inflammation in 3T3-L1 preadipocytes after 7 d exposure to selenite (Fig. 6). However, no effect was observed, indicating that selenite modulates the antioxidant status of the cells without affecting any key regulators of redox status or markers of energy metabolism and adipocytes differentiation.

Adipocyte differentiation was characterized in function of changes on markers of redox status, inflammation, and energy metabolism. In mature adipocytes, an increase in *Pparg*, *Cebpa* and *Fabp4* mRNA expression (ie, early markers of differentiation) was observed compared with preadipocytes, confirming the differentiation status of the cells and supporting previous study results showing that the maturation of 3T3-L1 adipocytes is characterized by the increase in the markers of adipocytes differentiation [28]. A significant decrease in *Gpx1* mRNA expression was observed, but no effect was observed on mRNA expression of regulators of redox status and inflammation, such as *Nrf2*, *Ho-1* or *Cox2*, compared with preadipocytes (Fig. 7). These results suggest that adipocytes maturation and lipid deposition are characterized by a decrease in antioxidant capacity of the cell (GPX1), even if no changes were observed at the level of gene expression for *Nrf2* transcription factor regulator of antioxidant defense and for the *Cox2* regulator of

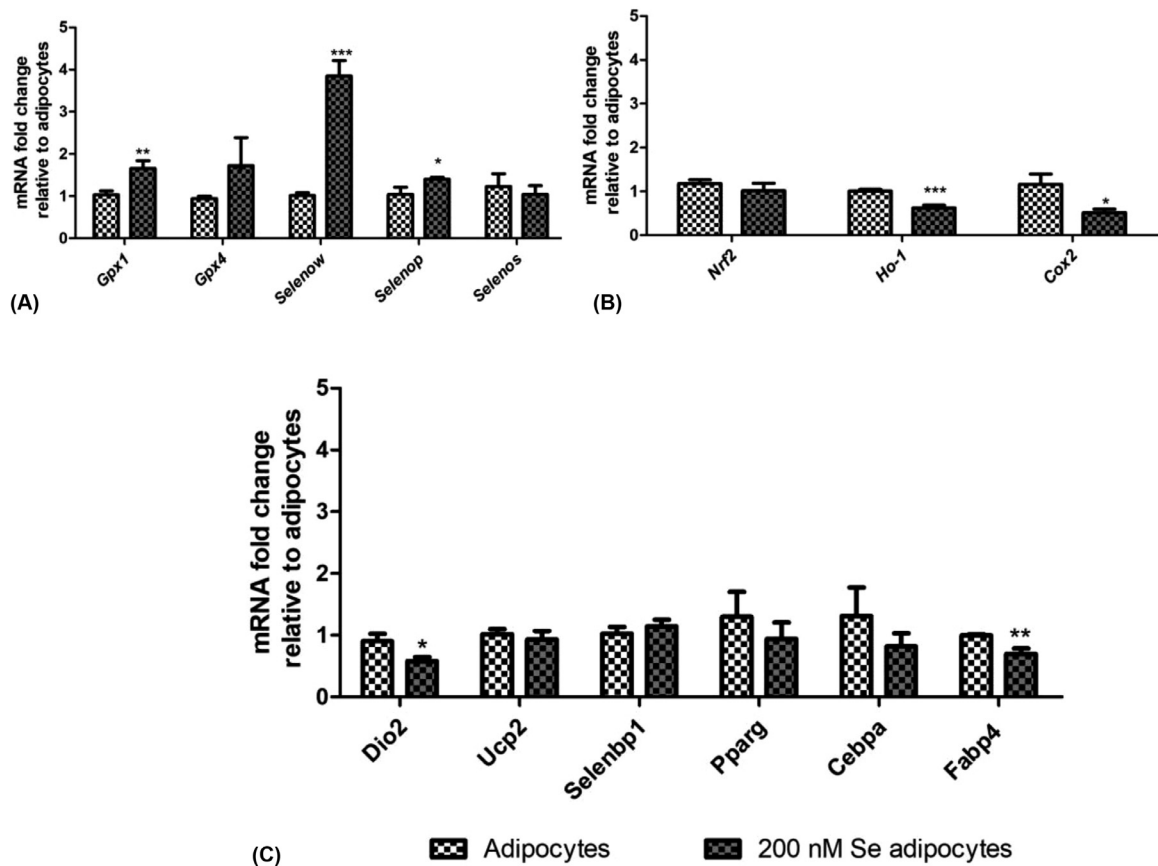


**Fig. 8.** Effect of 7 d exposure to 200 nM sodium selenite during differentiation on gene expression of (A) *Gpx1*, *Gpx4*, *Selenow*, *Selenop* and *Selenos*; (B) *Nrf2*, *Ho-1* and *Cox2*; and (C) *Dio2*, *Ucp2*, *Selenbp1*, *Pparg*, *Cebpa* and *Fabp4* in untreated adipocytes (adipocytes) and adipocytes exposed to 200 nM sodium selenite for 7 d (200 nM Se adipocytes;  $n = 3-7$ ). Data are expressed as fold change compared with untreated adipocytes (adipocytes). \* $P < 0.05$ ; \*\* $P < 0.01$ ; \*\*\* $P < 0.001$  versus adipocytes. *Cebpa*, CCAAT/enhancer binding protein alpha; *Cox2*, cyclooxygenase 2; *Dio2*, type II iodothyronine deiodinase; *Fabp4*, fatty acid binding protein 4; *Gpx1*, glutathione peroxidase 1; *Gpx4*, glutathione peroxidase 4; *Ho-1*, heme oxygenase 1; *Nrf2*, nuclear factor erythroid 2 related factor 2; *Pparg*, peroxisome proliferator activated receptor gamma; *Selenbp1*, selenium-binding protein P1; *Selenop*, selenoprotein P; *Selenos*, selenoprotein S; *Selenow*, selenoprotein W; *Ucp2*, uncoupling protein 2.

inflammation. Moreover, adipocyte maturation was characterized by an increase in *Dio2* and *Selenbp1* (Fig. 7), reflecting a decrease in lipid catabolism and increase in ROS production, respectively [26,27]. These results support the potential role of oxidative stress in lipid accumulation and preadipocytes differentiation, which was confirmed by a significant increase in intracellular ROS levels in adipocytes compared with preadipocytes (Fig. 5). Consistent with these results, a study by Kobayashi et al. showed that maturation of preadipocytes may be related to the increase in ROS, GPX was one of the antioxidant enzymes that was downregulated in hypertrophied adipose tissue, and its cellular activity was decreased during the maturation of 3T3-L1 preadipocytes [38].

To investigate the molecular mechanisms that are responsible for the decrease in adipocyte differentiation and lipid deposition induced by selenium and assessed by ORO staining (Fig. 3), the effect of 200 nM sodium selenite supplementation during the differentiation process on intracellular ROS levels and mRNA expression of different selenoproteins, markers of adipocytes differentiation, redox, and energy metabolism regulators and inflammation was assessed. Selenite supplementation during differentiation caused a decrease in intracellular ROS levels (Fig. 5), which was paralleled by an increase in *Gpx1*, *Selenow*, *Selenop* expressions, and a decrease in *Ho-1* mRNA expressions compared with non-supplemented adipocytes (Fig. 8). Moreover, the expression of markers of energy metabolism, inflammation, and adipocytes differentiation (eg, *Dio2*, *Cox2* and *Fabp4*) was significantly

reduced in adipocytes supplemented with selenite. These results are in agreement with previous publications, including by Kim et al. (2012) who stated that *Cebpa* mRNA was decreased during 3T3-L1 differentiation [43] whereas GPX1 and SELENOW in addition to SELENOH were shown to be the selenoproteins most affected by selenium in a dose-dependent manner in RAW264.7 cells after lipopolysaccharide stimulation [34].

From the results obtained in this study, the following mechanism can be proposed: selenium supplementation, as inorganic selenite, during differentiation causes a decrease in intracellular ROS levels that is matched by an increase in selenoprotein gene expression (*Gpx1*, *Selenow*, and *Selenop*), which induce an increase in antioxidant capacity and decrease in inflammatory mediators (*Cox2*) and subsequent decrease in energy metabolism and adipocyte differentiation markers (*Dio2* and *Fabp4*), subsequently affecting adipocyte differentiation and reducing lipid deposition. The decrease in *Ho-1* mRNA expression may be related to a feedback inhibition mechanism due to the increase in the antioxidant capacity of the cell due to selenium acting directly through selenoproteins (GPX1, SELENOW, and SELENOH; Fig. 9). To our knowledge, this is the first study to illustrate the underlying mechanism of selenite in 3T3-L1 cells through the modulation of *Gpx1*, *Selenow*, *Selenop*, *Ho-1*, *Dio2* and *Fabp4* expression.

Some limitations are associated with this study, which should be considered. The murine 3T3-L1 cell line is widely used as *in vitro* model, and well reflects the respective processes in primary



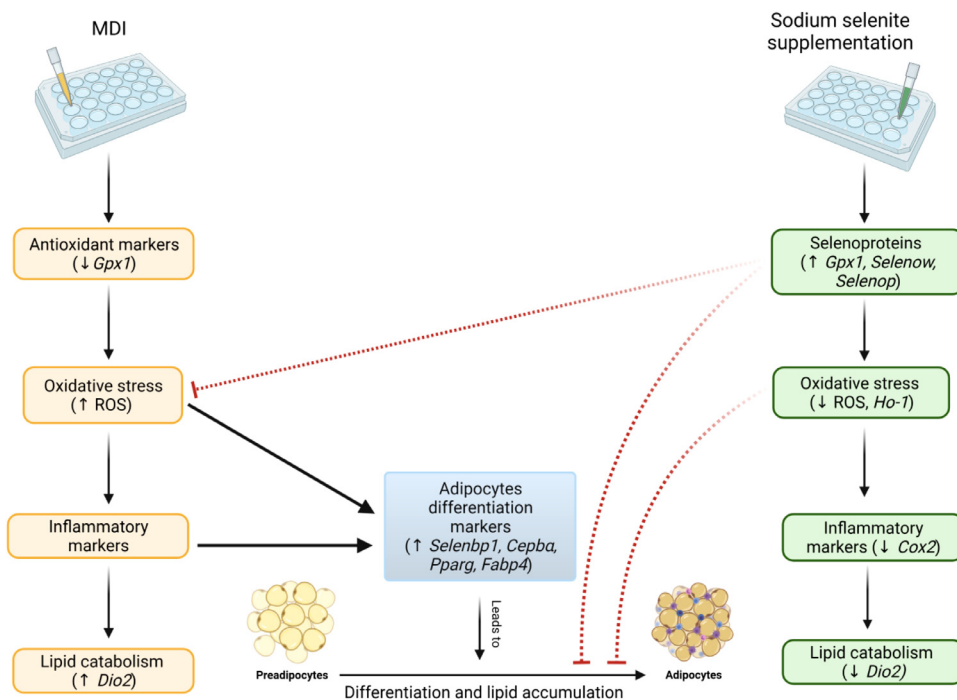


**Fig. 9.** Diagram of proposed mechanism for selenite modulation of adipogenesis. Selenite causes an increase in selenoprotein expression (*Gpx1*, *Selenow*, and *Selenop*) that induces an increase in the antioxidant capacity of the cells, decrease in inflammatory mediators (*Cox2*), and subsequent decrease in adipocytes differentiation markers (*Fabp4*) at the gene level, and, subsequently, affects adipocytes differentiation and lipid deposition. Created with BioRender.com. *Cebpa*, CCAAT/enhancer-binding protein alpha; *Cox2*, cyclooxygenase 2; *Dio2*, type II iodothyronine deiodinase; *Fabp4*, fatty acid binding protein 4; *Gpx1*, glutathione peroxidase 1; *Ho-1*, heme oxygenase 1; MDI, hormone mixture; *Pparg*, peroxisome proliferator activated receptor gamma; ROS, reactive oxygen species; *Selenop*, selenoprotein P; *Selenow*, selenoprotein W.

preadipocytes undergoing adipocyte differentiation, compared with some available cell lines, counteracting the translation of findings to humans. The concentration of sodium selenite chosen for this study (200 nM) reflects the optimal amount of selenium required for maximum *Gpx1* expression in this cell culture system and ensure saturated biosynthesis of selenoproteins [44]. However, more studies are required to better identify the underlying mechanisms that regulate the tight U-shape dose–response associated with selenium status and selenoprotein metabolism in adipocyte physiology and obesity pathogenesis [16].

## Conclusion

The present study indicates that adipogenesis, as indicated by an increase in expression of adipogenesis mediators (*Selenbp1*, *Pparg*, *Cebpa*, and *Fabp4*) and presence of lipid accumulation, is modulated by oxidative stress (decrease in antioxidant mediators [*Gpx1*] and increase in ROS levels) and by selenium supplementation. Selenium supplementation successfully prevented adipogenesis in an *in vitro* system, as indicated by the decrease in lipid accumulation and ROS levels (key signaling molecules driving differentiation), and we hypothesize this is mediated through the increase in antioxidant capacity of the cells (*Gpx1*, *Selenow*, and *Selenop*, decrease in inflammatory mediators (*Cox2*), and decrease in adipogenesis mediators (*Dio2* and *Fabp4*). If these findings are replicated *in vivo* and physiological relevance is demonstrated, they may provide valuable data for a novel dietary approach to prevent obesity.

In addition, the present findings provide an evidence-based rationale for dietary selenium supplementation of individuals whose selenium status is suboptimal, which might be very useful in obese patients infected with the coronavirus disease of 2019 (COVID-19), because recent studies have revealed that selenium

status plays an important role in determining the host response to viral infections, and more specifically to severe acute respiratory syndrome coronavirus 2 (SARS-CoV-2) infection [45–48]. SARS-CoV-2 binds to the angiotensin converting enzyme 2 (ACE2) receptor that is expressed in adipose tissue and, therefore, presents at higher quantities in obese individuals; thus, strategies that may reduce adipogenesis, such as the proposed role for selenium might be important to study in light of the two current world epidemics (ie, obesity and COVID-19). In addition, GPX1, which is affected by selenium concentrations, has been identified as having an important role in SARS-CoV-2 infection. In addition to minimizing the effects of oxidative stress, GPX1 appears to interact with the M<sup>PTD</sup>, a protein responsible for cleaving polyproteins that are involved with the virus' structural components, blocking one of the primordial steps for the viral reproduction cycle [49].

## Acknowledgments

Dr NF Abo El-Magd was supported by Egyptian Government scholarship fund from the Egyptian Cultural and Educational Bureau, and the work was supported by the Centre for Obesity Research and Education, Robert Gordon University in Aberdeen, United Kingdom.

## References

- [1] DeFronzo RA, Ferrannini E, Groop L, Henry RR, Herman WH, Holst JJ, et al. Type 2 diabetes mellitus. *Nat Rev Dis Primers* 2015;1:15019.
- [2] Malik VS, Willett WC, Hu FB. Global obesity: trends, risk factors and policy implications. *Nat Rev Endocrinol* 2013;9:13–27.
- [3] Spiegelman BM, Flier JS. Obesity and the regulation of energy balance. *Cell* 2001;104:531–43.
- [4] Keane JF Jr, Larson MG, Vasan RS, Wilson PW, Lipinska I, Corey D, et al. Obesity and systemic oxidative stress: clinical correlates of oxidative stress in the Framingham Study. *Arterioscler Thromb Vasc Biol* 2003;23:434–9.

- [5] Manna P, Jain SK. Obesity, oxidative stress, adipose tissue dysfunction, and the associated health risks: causes and therapeutic strategies. *Metab Syndr Relat Disord* 2015;13:423–44.
- [6] Zhang Y, Chen X. Reducing selenoprotein P expression suppresses adipocyte differentiation as a result of increased preadipocyte inflammation. *Am J Physiol Endocrinol Metab* 2011;300:E77–85.
- [7] Spalding KL, Amer E, Westermarck PO, Bernard S, Buchholz BA, Bergmann O, et al. Dynamics of fat cell turnover in humans. *Nature* 2008;453:783–7.
- [8] Fang DL, Wan Y, Shen W, Cao J, Sun ZX, Yu HH, et al. Endoplasmic reticulum stress leads to lipid accumulation through upregulation of SREBP-1c in normal hepatic and hepatoma cells. *Mol Cell Biochem* 2013;381:127–37.
- [9] Sekiya M, Hiraishi A, Touyama M, Sakamoto K. Oxidative stress induced lipid accumulation via SREBP1c activation in HepG2 cells. *Biochem Biophys Res Commun* 2008;375:602–7.
- [10] Lee J, Homma T, Kurahashi T, Kang ES, Fujii J. Oxidative stress triggers lipid droplet accumulation in primary cultured hepatocytes by activating fatty acid synthesis. *Biochem Biophys Res Commun* 2015;464:229–35.
- [11] Zhao X, Hu H, Wang C, Bai L, Wang Y, Wang W, et al. A comparison of methods for effective differentiation of the frozen-thawed 3T3-L1 cells. *Anal Biochem* 2019;568:57–64.
- [12] Schwarz M, Lossow K, Kopp JF, Schwerdtle T, Kipp AP. Crosstalk of NRF2 with the trace elements selenium, iron, zinc, and copper. *Nutrients* 2019;11.
- [13] Ortega RM, Rodriguez-Rodriguez E, Aparicio A, Jimenez-Ortega AI, Palmeros C, Perea JM, et al. Young children with excess of weight show an impaired selenium status. *Int J Vitam Nutr Res* 2012;82:121–9.
- [14] Strauss RS. Comparison of serum concentrations of alpha-tocopherol and beta-carotene in a cross-sectional sample of obese and nonobese children (NHANES III). National Health and Nutrition Examination Survey. *J Pediatr* 1999;134:160–5.
- [15] Kaidar-Person O, Person B, Szomstein S, Rosenthal RJ. Nutritional deficiencies in morbidly obese patients: a new form of malnutrition? Part B: minerals. *Obes Surg* 2008;18:1028–34.
- [16] Tinkov AA, Ajsuvakova OP, Filippini T, Zhou JC, Lei XG, Gatiatulina ER, et al. Selenium and selenoproteins in adipose tissue physiology and obesity. *Biomolecules* 2020;10.
- [17] Tang X, Li J, Zhao WG, Sun H, Guo Z, Jing L, et al. Comprehensive map and functional annotation of the mouse white adipose tissue proteome. *Peer J* 2019;7:e7352.
- [18] Zhao H, Li K, Tang JY, Zhou JC, Wang KN, Xia XJ, et al. Expression of selenoprotein genes is affected by obesity of pigs fed a high-fat diet. *J Nutr* 2015;145:1394–401.
- [19] Hatfield DL, Gladyshev VN. How selenium has altered our understanding of the genetic code. *Mol Cell Biol* 2002;22:3565–76.
- [20] Kim CY, Kim KH. Selenate prevents adipogenesis through induction of selenoprotein S and attenuation of endoplasmic reticulum stress. *Molecules* 2018;23.
- [21] Birringer M, Pilawa S, Flohe L. Trends in selenium biochemistry. *Nat Prod Rep* 2002;19:693–718.
- [22] Papp LV, Lu J, Holmgren A, Khanna KK. From selenium to selenoproteins: Synthesis, identity, and their role in human health. *Antioxid Redox Signal* 2007;9:775–806.
- [23] Fairweather-Tait SJ, Bao Y, Broadley MR, Collings R, Ford D, Hesketh JE, et al. Selenium in human health and disease. *Antioxid Redox Signal* 2011;14:1337–83.
- [24] Steinbrenner H, Sies H. Protection against reactive oxygen species by selenoproteins. *Biochim Biophys Acta* 2009;1790:1478–85.
- [25] Barnes KM, Evenson JK, Raines AM, Sunde RA. Transcript analysis of the selenoproteome indicates that dietary selenium requirements of rats based on selenium-regulated selenoprotein mRNA levels are uniformly less than those based on glutathione peroxidase activity. *J Nutr* 2009;139:199–206.
- [26] Bradley D, Liu J, Blaszczyk A, Wright V, Jalilvand A, Needleman B, et al. Adipocyte DIO2 expression increases in human obesity but is not related to systemic insulin sensitivity. *J Diabetes Res* 2018;2018:2464652.
- [27] Steinbrenner H, Micoogullari M, Hoang NA, Bergheim I, Klotz LO, Sies H. Selenium-binding protein 1 (SELENBP1) is a marker of mature adipocytes. *Redox Biol* 2019;20:489–95.
- [28] Chen J, Bao C, Kim JT, Cho JS, Qiu S, Lee HJ. Sulforaphane inhibition of adipogenesis via hedgehog signaling in 3T3-L1 adipocytes. *J Agric Food Chem* 2018;66:11926–34.
- [29] Zebisch K, Voigt V, Wabitsch M, Brandsch M. Protocol for effective differentiation of 3T3-L1 cells to adipocytes. *Anal Biochem* 2012;425:88–90.
- [30] Shim EH, Lee H, Lee MS, You S. Anti-adipogenic effects of the traditional herbal formula Dohongsamul-tang in 3T3-L1 adipocytes. *BMC Complement Altern Med* 2017;17:542.
- [31] Koh EJ, Kim KJ, Seo YJ, Choi J, Lee BY. Modulation of HO-1 by ferulic acid attenuates adipocyte differentiation in 3T3-L1 cells. *Molecules* 2017;22.
- [32] Choi HS, Kim JW, Cha YN, Kim C. A quantitative nitroblue tetrazolium assay for determining intracellular superoxide anion production in phagocytic cells. *J Immunoassay Immunochem* 2006;27:31–44.
- [33] Ball HJ, MacDougall HG, McGregor IS, Hunt NH. Cyclooxygenase-2 in the pathogenesis of murine cerebral malaria. *J Infect Dis* 2004;189:751–8.
- [34] Wang L, Jing J, Yan H, Tang J, Jia G, Liu G, et al. Selenium pretreatment alleviated LPS-induced immunological stress via upregulation of several selenoprotein encoding genes in murine RAW264.7 cells. *Biol Trace Elem Res* 2018;186:505–13.
- [35] Pieralisi A, Martini C, Soto D, Vila MC, Calvo JC, Guerra LN. N-acetylcysteine inhibits lipid accumulation in mouse embryonic adipocytes. *Redox Biol* 2016;9:39–44.
- [36] Calzadilla P, Sapochnik D, Cosentino S, Diz V, Dixelio L, Calvo JC, et al. N-acetylcysteine reduces markers of differentiation in 3T3-L1 adipocytes. *Int J Mol Sci* 2011;12:6936–51.
- [37] Araki S, Dobashi K, Kubo K, Yamamoto Y, Asayama K, Shirahata A. N-acetylcysteine attenuates TNF-alpha induced changes in secretion of interleukin-6, plasminogen activator inhibitor-1 and adiponectin from 3T3-L1 adipocytes. *Life Sci* 2006;79:2405–12.
- [38] Kobayashi H, Matsuda M, Fukuhara A, Komuro R, Shimomura I. Dysregulated glutathione metabolism links to impaired insulin action in adipocytes. *Am J Physiol Endocrinol Metab* 2009;296:E1326–34.
- [39] Weiss Sachdev S, Sunde RA. Selenium regulation of transcript abundance and translational efficiency of glutathione peroxidase-1 and -4 in rat liver. *Biochem J* 2001;357:851–8.
- [40] Wingle K, Bocher M, Flohe L, Kollmus H, Brigelius-Flohe R. mRNA stability and selenocysteine insertion sequence efficiency rank gastrointestinal glutathione peroxidase high in the hierarchy of selenoproteins. *Eur J Biochem* 1999;259:149–57.
- [41] Brigelius-Flohe R. Tissue-specific functions of individual glutathione peroxidases. *Free Radic Biol Med* 1999;27:951–65.
- [42] Kipp A, Banning A, van Schothorst EM, Meplan C, Schomburg L, Evelo C, et al. Four selenoproteins, protein biosynthesis, and Wnt signalling are particularly sensitive to limited selenium intake in mouse colon. *Mol Nutr Food Res* 2009;53:1561–72.
- [43] Kim CY, Kim GN, Wiacek JL, Chen CY, Kim KH. Selenate inhibits adipogenesis through induction of transforming growth factor-beta1 (TGF-beta1) signaling. *Biochem Biophys Res Commun* 2012;426:551–7.
- [44] Leist M, Raab B, Maurer S, Rosick U, Brigelius-Flohe R. Conventional cell culture media do not adequately supply cells with antioxidants and thus facilitate peroxide-induced genotoxicity. *Free Radic Biol Med* 1996;21:297–306.
- [45] Bermano G, Meplan C, Mercer DK, Hesketh JE. Selenium and viral infection: are there lessons for COVID-19? *Br J Nutr* 2021;125:618–27.
- [46] Alexander J, Tinkov A, Strand TA, Alehagen U, Skalny A, Aaseth J. Early nutritional interventions with zinc, selenium and vitamin D for raising anti-viral resistance against progressive COVID-19. *Nutrients* 2020;12.
- [47] Zhang J, Taylor EW, Bennett K, Saad R, Rayman MP. Association between regional selenium status and reported outcome of COVID-19 cases in China. *Am J Clin Nutr* 2020;111(6):1297–9.
- [48] Jayawardena R, Sooriyaarachchi P, Chourdakis M, Jeewandara C, Ranasinghe P. Enhancing immunity in viral infections, with special emphasis on COVID-19: A review. *Diabetes Metab Syndr* 2020;14:367–82.
- [49] Seale LA, Torres DJ, Berry MJ, Pitts MW. A role for selenium-dependent GPX1 in SARS-CoV-2 virulence. *Am J Clin Nutr* 2020;112:447–8.